SUPPORTING INFORMATION

Polysaccharide succinylation enhances the intracellular survival of *Mycobacterium abscessus*

Zuzana Palčeková[1], Martine Gilleron[2], Shiva kumar Angala[1], Juan Manuel Belardinelli[1], Michael McNeil[1], Luiz E. Bermudez[3,4], Mary Jackson[1*]

From the [1]Mycobacteria Research Laboratories, Department of Microbiology, Immunology and Pathology, Colorado State University, Fort Collins, CO 80523-1682, USA; [2]Institut de Pharmacologie et de Biologie Structurale, IPBS, Université de Toulouse, CNRS, UPS, 31077 Toulouse, France; [3]Department of Biomedical Sciences, College of Veterinary Medicine, Oregon State University, Corvallis, OR 97331, USA; [4]Department of Microbiology, College of Science, Oregon State University, Corvallis, OR 97331, USA

[*]Corresponding Author: Mary Jackson; Mary.Jackson@colostate.edu

Table of contents

Figure S3: Absence of capping motifs in *Mabs* LAM.

Figure S4: Primary sequence alignment of SucT from *M. tuberculosis* H37Rv (Rv1565c), *M. smegmatis* mc^2155 (MSMEG_3187) and *M. abscessus* ATCC 19977 (MAB_2689) using PSI/TM-Coffee.

Figure S5: Allelic replacement at the *MAB_2689* locus of *Mabs* ATCC 19977.

Figure S6: Congo red does not bind to *Mabs* WT and Δ*sucT* LAM.

Figure S7: Phenotypic characterization of the *Mabs sucT* mutant.

Figure S8: Effect of reactive oxygen species and phagosome acidification on the intracellular replication and survival of the *Mabs sucT* knock-out mutant.

Table S1: Monosaccharidic composition of LM and LAM from WT *Mabs* ATCC 19977, the Δ*sucT* mutant and the complemented mutant strain.
Reported values are averages ± standard deviations of three technical repeats and represent relative distribution in %.

(A) Monosaccharidic composition of LAM

	Ara*f*	Ino	Man*p*	2-*O*-methyl-Man*p*	Ara*f*/Man*p*
WT	78.0 ± 1.2	0.5 ± 0.1	20.3 ± 1.4	1.2 ± 0.3	3.6 ± 0.3
Δ*sucT*	81.3 ± 1.1	0.5 ± 0.1	17.1 ± 1.3	1.0 ± 0.2	4.5 ± 0.4
Δ*sucT* comp	78.2 ± 0.6	0.4 ± 0.1	19.9 ± 0.6	1.5 ± 0.2	3.7 ± 0.1

The LAMs produced by the three strains show no statistically significant difference in Ara*f*/Man*p* ratio pursuant to the Student's *t*-test ($P < 0.05$).

(B) Monosaccharidic composition of LM

	Ino	Man*p*	2-*O*-methyl-Man*p*
WT	1.5 ± 0.5	95.6 ± 1.1	2.9 ± 0.7
Δ*sucT*	1.5 ± 0.6	95.1 ± 0.5	3.4 ± 0.7
Δ*sucT* comp	2.3 ± 0.5	94.6 ± 0.6	3.1 ± 0.2

Table S2: Glycosyl linkage analysis of per-*O*-methylated LM and LAM from WT *Mabs* ATCC 19977, the Δ*sucT* mutant and the complemented mutant strain.
Reported values are averages ± SD of three technical repeats and represent relative distribution in %.

(A) Glycosyl linkage analysis of per-*O*-methylated LAM[a]

	t-Ara*f*	2-Ara*f*	5-Ara*f*	3,5-Ara*f*	t-Man*p*	6-Man*p*	3,6-Man*p*[b]	Ara*f*/Man*p*	3,6-Man*p*/6-Man*p*	2-Ara*f*/5-Ara*f*
WT	9.5 ± 1.0	6.4 ± 0.3	45.8 ± 0.8	14.7 ± 0.5	10.1 ± 0.7	7.2 ± 0.3	6.3 ± 0.1	3.1 ± 0.1	0.9	0.14 ± 0.01
Δ*sucT*	10.2 ± 1.3	8.2 ± 0.5	46.0 ± 0.8	11.7 ± 1.1	13.9 ± 0.4	5.1 ± 0.5	4.8 ± 0.3	4.2 ± 0.5	0.9	0.18 ± 0.01
Δ*sucT* comp	14.0 ± 1.2	8.1 ± 0.9	37.0 ± 1.1	14.6 ± 0.5	10.3 ± 0.2	7.5 ± 0.5	8.5 ± 1.2	2.7 ± 0.3	1.1	0.22 ± 0.02

[a]The LAM produced by the three strains show no statistically significant differences in terms of glycosyl linkages of their mannan and arabinan domains pursuant to the Student's *t*-test ($P < 0.05$). [b]2,6 linked Man*p* was found in small variable amounts (less than 16% of the 3,6-Man*p*). We attribute this to under methylation as 2,6-Man*p* could not be detected in the NMR analysis.

(B) Glycosyl linkage analysis of per-*O*-methylated LM[a]

	t-Man*p*	6-Man*p*	3,6-Man*p*[b]	3,6-Man*p*/6-Man*p*
WT	52.3 ± 3.7	20.5 ± 1.7	27.2 ± 2.7	1.3
Δ*sucT*	55.5 ± 1.0	18.0 ± 1.3	26.5 ± 0.7	1.5
Δ*sucT* comp	46.0 ± 1.0	20.4 ± 0.6	33.6 ± 0.9	1.6

[a]The LM produced by the three strains show no statistically significant differences in terms of glycosyl linkages of their mannan domain pursuant to the Student's *t*-test ($P < 0.05$). [b]2,6 linked Man*p* was found in small variable amounts (less than 16% of the 3,6-Man*p*). We attribute this to under methylation as 2,6-Man*p* could not be detected in the NMR analysis.

Table S3: Fatty acid composition of the mannosylated phosphatidyl-*myo*-inositol anchor of LM and LAM from WT *Mabs* ATCC 19977 and the Δ*sucT* knockout mutant.

Reported values represent relative distribution in %. TBSA: Tuberculostearic acid.

	C14:0	C15:0	C16:0	C18:1	C18:0	C19:0 (TBSA)
LM WT	0.9	0.7	36.20	6.40	32.9	22.9
LM Δ*sucT*	1.2	0.4	34.6	1.6	45.8	16.4
LAM WT	14.2	1.5	66.1	1.1	9.1	8.0
LAM Δ*sucT*	9.0	1.5	57.1	4.8	20.6	7.0

Table S4: Relative percentage of Ara_4 and Ara_6 oligoarabinosides released upon *Cellulomonas gelida* endoarabinanase digestion and the individual representation (%) of covalently modified oligoarabinosides within each group.

	WT	Δ*sucT*	Δ*sucT* comp
Total Ara_4	**50.2**	**38.6**	**52.4**
Unmodified Ara_4	77	95.8	80.8
Ara_4+succinate	14.5	0	13.4
Ara_4+acetate	7.6	4.2	5.2
Ara_4+succinate+acetate	0.9	0	0.6
Total Ara_6	**49.8**	**61.4**	**47.6**
Unmodified Ara_6	86.9	98.4	88.3
Ara_6+succinate	5.8	0	6.6
Ara_6+acetate	7.3	1.6	5.0
Ara_6+succinate+acetate	0	0	0.1
SUM	**100**	**100**	**100**

Table S5: Monosaccharidic composition of mAGP from WT *Mabs* ATCC 19977, the Δ*sucT* mutant and the complemented mutant strain. Reported values are averages ± SD of three technical repeats and represent relative distribution in %. No statistically significant differences between strains were observed pursuant to the Student's *t*-test ($P < 0.05$).

	Rha*p*	Ara*f*	Gal*f*	GlcNAc	MurNAc	Ara*f*/Gal*f*	Ara*f*/Rha*p*	Gal*f*/Rha*p*	mycolic acids/Rha*p*
WT	1.1 ± 0.1	46.0 ± 2.3	22.5 ± 2.0	10.5 ± 1.2	15.2 ± 3.3	2.1 ± 0.1	43.0 ± 5.1	20.9 ± 2.8	25.4 ± 9.8
Δ*sucT*	1.2 ± 0.1	47.8 ± 1.6	18.9 ± 1.1	11.2 ± 2.1	15.7 ± 3.1	2.5 ± 0.2	39.5 ± 0.8	15.7 ± 1.5	34.6 ± 3.7
Δ*sucT* comp	1.2 ± 0.3	45.4 ± 2.1	20.4 ± 0.9	12.5 ± 3.9	19.7 ± 1.0	2.2 ± 0.1	39.8 ± 11.5	17.8 ± 4.9	37.9 ± 3.8

<u>Table S6</u>: Glycosyl linkage analysis of per-*O*-methylated mAGP from WT *Mabs* ATCC 19977, the Δ*sucT* mutant and the complemented mutant strain.

Reported values are averages ± SD of three technical repeats and represent relative distribution in %. No statistically significant differences between strains were observed pursuant to the Student's *t*-test ($P < 0.05$).

	t-Ara*f*	2-Ara*f*	5-Ara*f*	3,5-Ara*f*	t-Gal*f*	5-Gal*f*	6-Gal*f*	5,6-Gal*f*	Ara*f*/Gal*f*
WT	7.0 ± 0.3	6.0 ± 0.1	36.7 ± 0.9	9.7 ± 0.6	3.7 ± 0.3	20.2 ± 0.9	11.6 ± 0.8	4.5 ± 0.7	1.5 ± 0.1
Δ*sucT*	7.6 ± 0.8	5.3 ± 0.9	41.5 ± 3.5	8.2 ± 1.4	2.8 ± 0.6	19.1 ± 1.2	11.2 ± 1.1	3.8 ± 0.8	1.7 ± 0.2
Δ*sucT* comp	7.2 ± 0.3	5.8 ± 0.2	38.2 ± 0.7	9.5 ± 0.4	3.1 ± 0.2	19.3 ± 0.5	11.4 ± 0.5	4.6 ± 0.4	1.6 ± 0.1

Table S7: **Susceptibility of the *Mabs sucT* knock-out mutant to antibiotics and antimicrobial peptides.** MIC were determined in cation-adjusted Mueller-Hinton II broth + 0.05% tyloxapol at 37°C and MIC values are given in μg mL^{-1}. AMK, amikacin; APR, apramycin; AZI, azithromycin; CLA, clarithromycin; ERY, erythromycin; KAN, kanamycin; EMB, ethambutol; RIF, rifampicin; STR, streptomycin; CFX, cefoxitin; TOB, tobramycin; LIN, linezolid; TET, tetracycline; IMI, imipenem; CIP, ciprofloxacin. LL-37 (InvivoGen) and HNP-1 (human α-defensin 1; Bachem) are cationic antimicrobial peptides. MIC determinations were performed two times on independent culture batches. nd, not determined.

Antibiotic	*Mabs* WT	*Mabs*Δ*sucT*	*Mabs*Δ*sucT*/ pMV306-*sucT*
AMK	10	10	10
APR	2.5	2.5	2.5
AZI	40	80	40
CLA	0.63	0.63	0.63
ERY	5	5	5
KAN	10	10	nd
EMB	>320	>320	>320
RIF	>160	>160	>160
STR	160	160	80
CFX	80	40	80
TOB	40	80	40
LIN	10	5	10
TET	>320	>320	>320
IMI	20	20	20
CIP	5	5	5
LL-37	>100	>100	>100
HNP-1	>100	>100	>100

Table S8: **Translocation of *Mabs* WT, Δ*sucT* and complemented Δ*sucT* mutant strains across polarized monolayers of human A549 lung alveolar type II epithelial cells.**

No significant difference in translocation after 24 h was observed between mutant and WT or complemented mutant strains ($p>0.05$). Statistical analysis using 2-way ANOVA.

	CFU in the upper chamber	CFU recovered in the basal chamber after 24 h	% of inoculum that translocated after 24 h	Transmembrane potential (Ω/cm^2)
WT	$5.6 \pm 0.6 \times 10^6$	$1.1 \pm 0.8 \times 10^3$	0.020	254
Δ*sucT*	$5.0 \pm 0.4 \times 10^6$	$8.7 \pm 0.6 \times 10^2$	0.017	246
Δ*sucT* comp	$4.3 \pm 0.9 \times 10^6$	$8.9 \pm 0.5 \times 10^2$	0.020	251

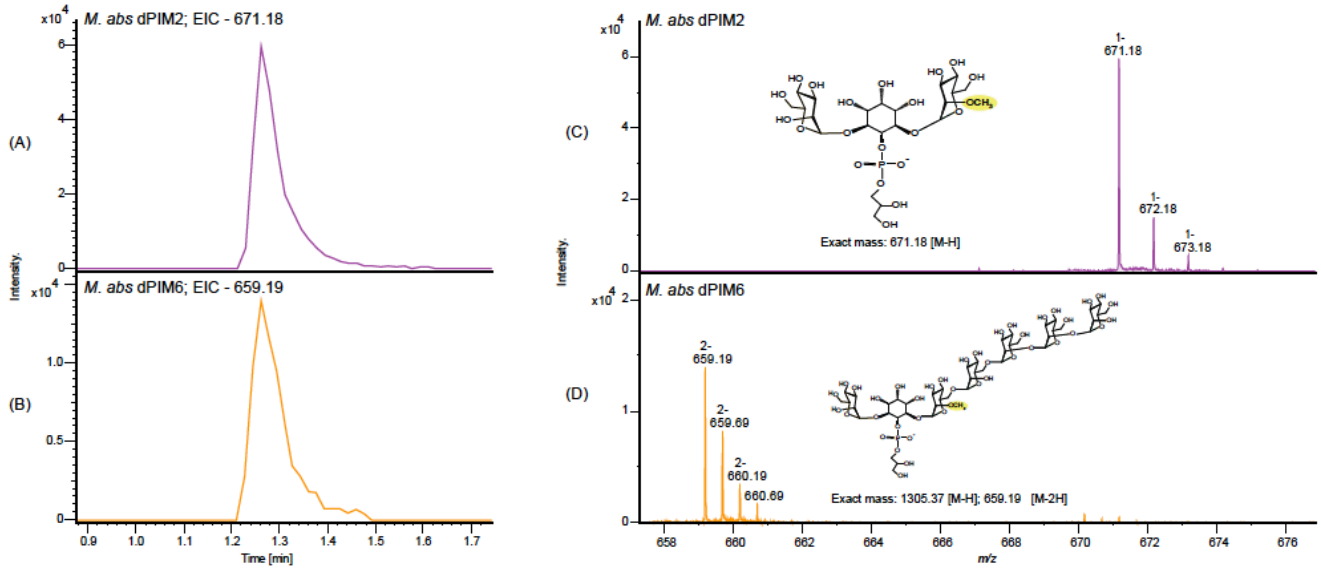

<u>Figure S1</u>: Negative ion liquid chromatography-mass spectrometry (LC-MS) analysis of *Mabs* deacylated PIM_2 (d-PIM_2) and deacylated PIM_6 (d-PIM_6).
(A, B) Extracted ion chromatograms (EICs) for d-PIM_2 (A) and d-PIM_6 (B) with *m/z* values of 671.18 and 659.19, respectively. (C, D) The mass spectra showing the singly charged [M-H] for d-PIM_2 (C), and doubly charged [M-2H] for d-PIM_6 (D). The chemical structures with exact mass corresponding to the methylated forms of d-PIM_2 (C) and d-PIM_6 (D) are shown.

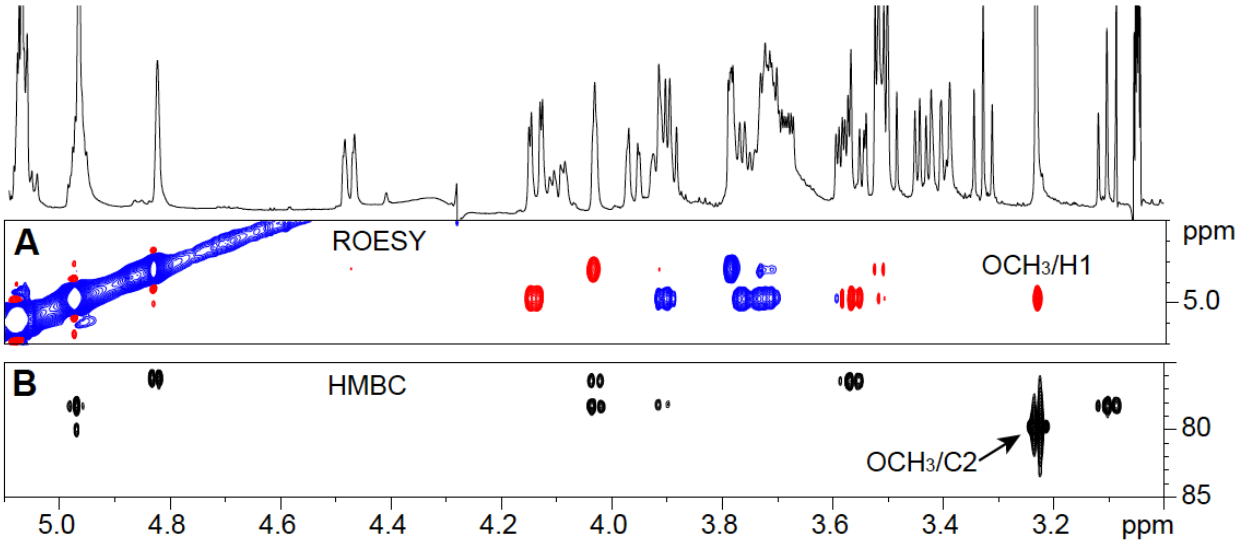

Figure S2: Location of the methyl group on *Mabs* tetra-acylated PIM_2.
Expanded regions of the 2D ^{1}H-^{1}H ROESY (δ ^{1}H 5.10-3.00 and δ ^{1}H 5.20-4.60) (A) and of the 2D ^{1}H-^{13}C HMBC (δ ^{1}H: 5.10-3.00, δ ^{13}C 85-75) (B) NMR spectra of the Ac_2PIM_2 from WT *Mabs* ATCC 19977 in $CDCl_3/CD_3OD/D_2O$, 60:35:8 (v/v/v) at 298 K.
On the ROESY spectrum (A), noe contacts are in red, while cosy contacts are in blue. The two important cross peaks allowing the location of the methyl group are annotated.

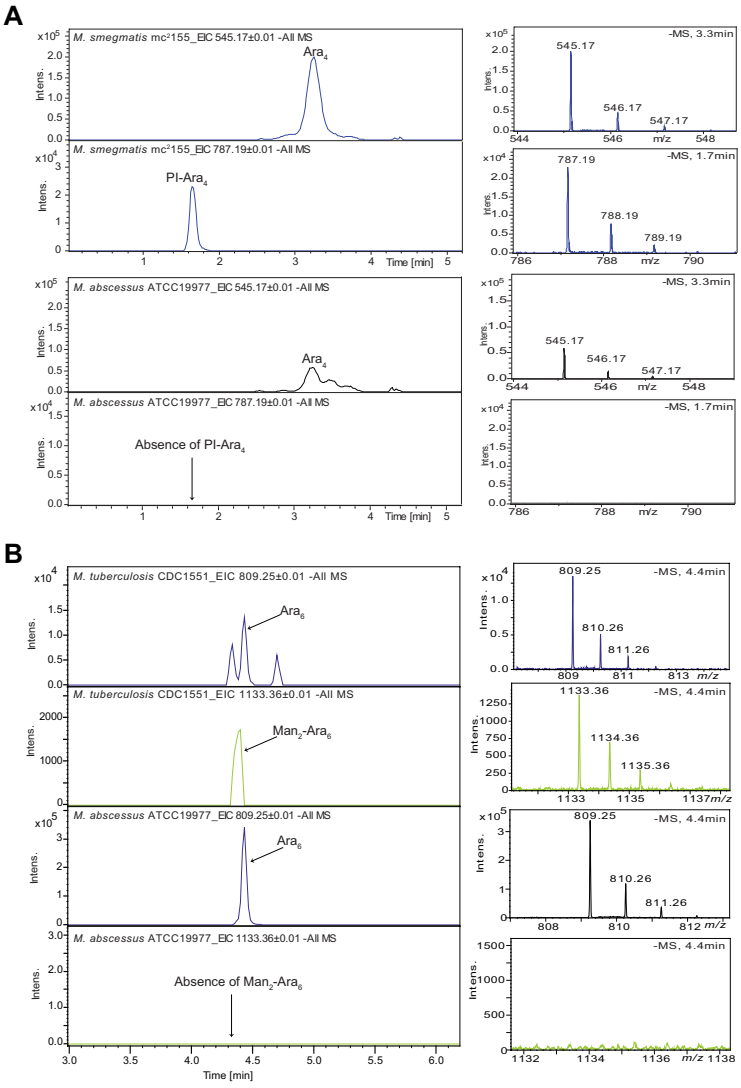

<u>Figure S3</u>: Absence of capping motifs in *Mabs* LAM.
The most abundant capped digestion product cleaved by *Cellulomonas gelida* endoarabinanase from the nonreducing end of LAM from *M. smegmatis* (A) and *M. tuberculosis* (B) is, respectively, phosphoinositol-Ara_4 with an exact mass of *m/z* 787.1915 $[M\text{-}H]^-$ and Man_2-Ara_6 with an exact mass of *m/z* 1133.36 $[M\text{-}H]^-$. None of these ions were detected in digested *Mabs* LAM (panels A and B). Three signals at similar retention times with an exact mass of *m/z* 545.1723 $[M\text{-}H]^-$ corresponding to Ara_4 were found in the digested *Mabs* LAM which reveals the possibility of more structural isomers of tetraarabinosides released by *Cellulomonas gelida* endoarabinanase.

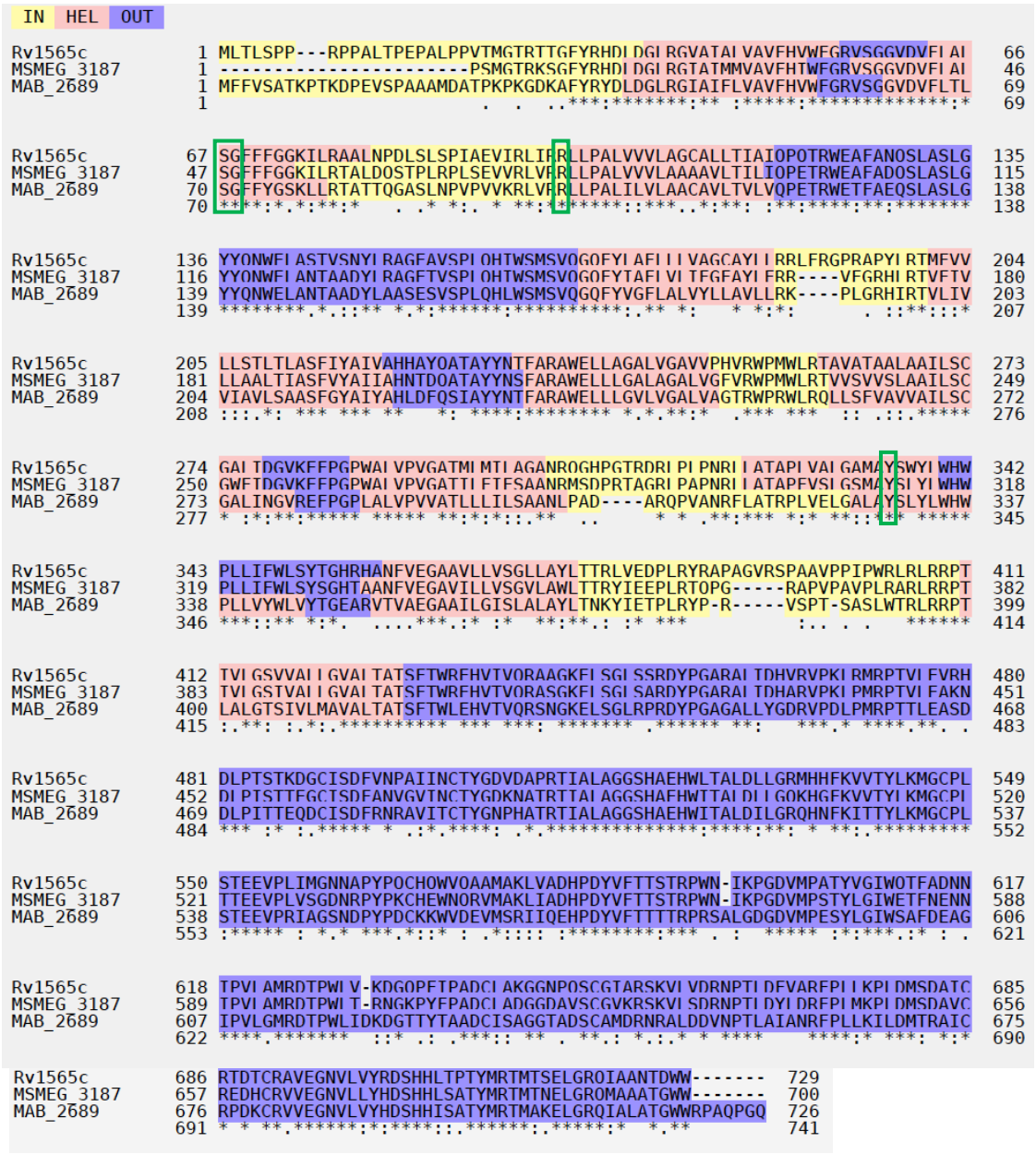

Figure S4: Primary sequence alignment of SucT from *M. tuberculosis* H37Rv (Rv1565c), *M. smegmatis* mc²155 (MSMEG_3187) and *M. abscessus* ATCC 19977 (MAB_2689) using PSI/TM-Coffee.

Conserved sequence (*), conservative mutations (:), semi-conservative mutations (.), and non-conservative mutations ( ). Predicted essential functional residues for catalytic activity are boxed in green.

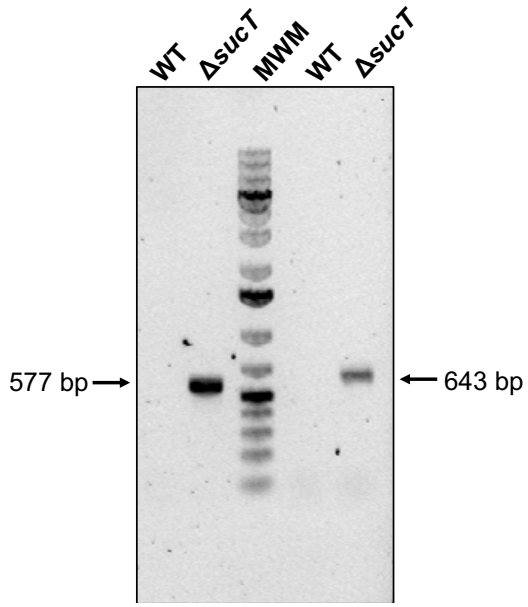

Figure S5: Allelic replacement at the *MAB_2689* locus of *Mabs* ATCC 19977.
Allelic replacement at the *MAB_2689* locus was confirmed by PCR using sets of primers located outside the allelic exchange substrates and inside the zeocin resistance cassette. The expected sizes of the PCR amplification products in the knock-out mutant are 577-bp for the upstream region of the deleted gene and 643-bp for the downstream region. No amplification was expected in the WT parent strain.

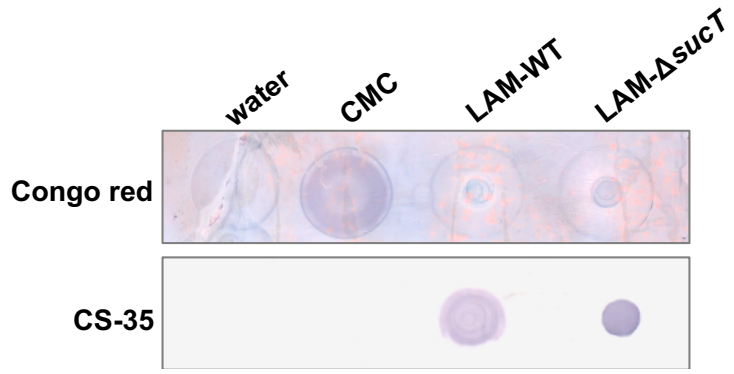

<u>Figure S6</u>: Congo red does not bind to *Mabs* WT and Δ*sucT* LAM.
Equal amounts of LAM from the WT and Δ*sucT* mutant strains were dot-blotted on the nitrocellulose membrane and stained with Congo red. Carboxymethylcellulose (CMC) (same amount loaded as for LAM) was used as a positive control for Congo red binding. LAM from the WT and mutant strains failed to react with Congo Red while they reacted, as expected, with the anti-LAM antibody CS-35.

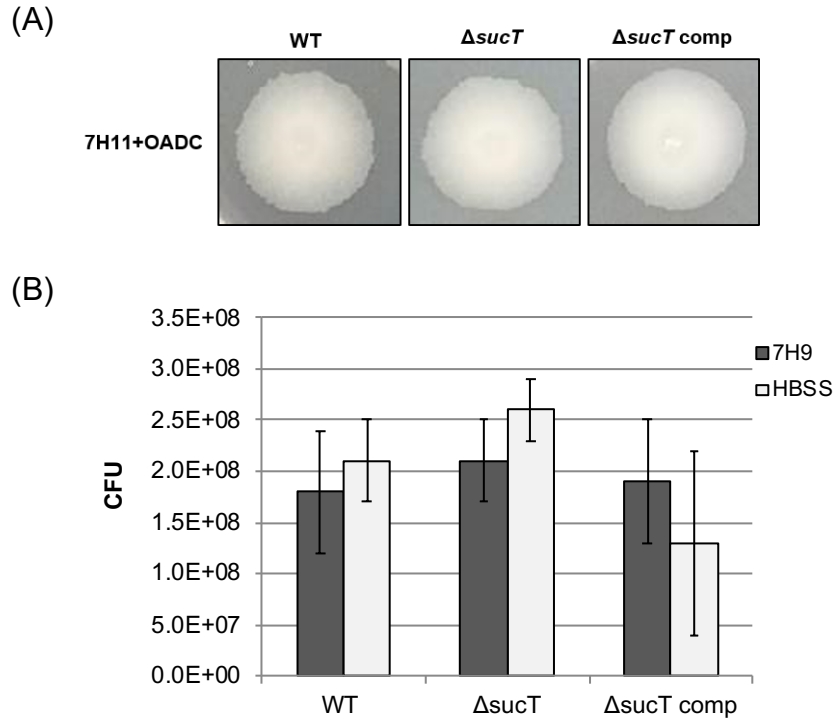

Figure S7: Phenotypic characterization of the *Mabs sucT* mutant.
(A) Colony morphology of WT *Mabs* ATCC 19977, the Δ*sucT* mutant and the complemented mutant strain after 3 day of incubation on 7H11-OADC agar at 37°C.
(B) Comparison of the ability of WT *Mabs* ATCC 19977, the Δ*sucT* mutant and the complemented mutant strain to form static biofilms in Hank's balanced salt solution (HBSS) and 7H9-OADC culture medium. No statistically significant differences in biofilm formation, neither in 7H9-OADC or HBSS buffer, were observed between strains pursuant to Student's *t*-test ($P < 0.05$).

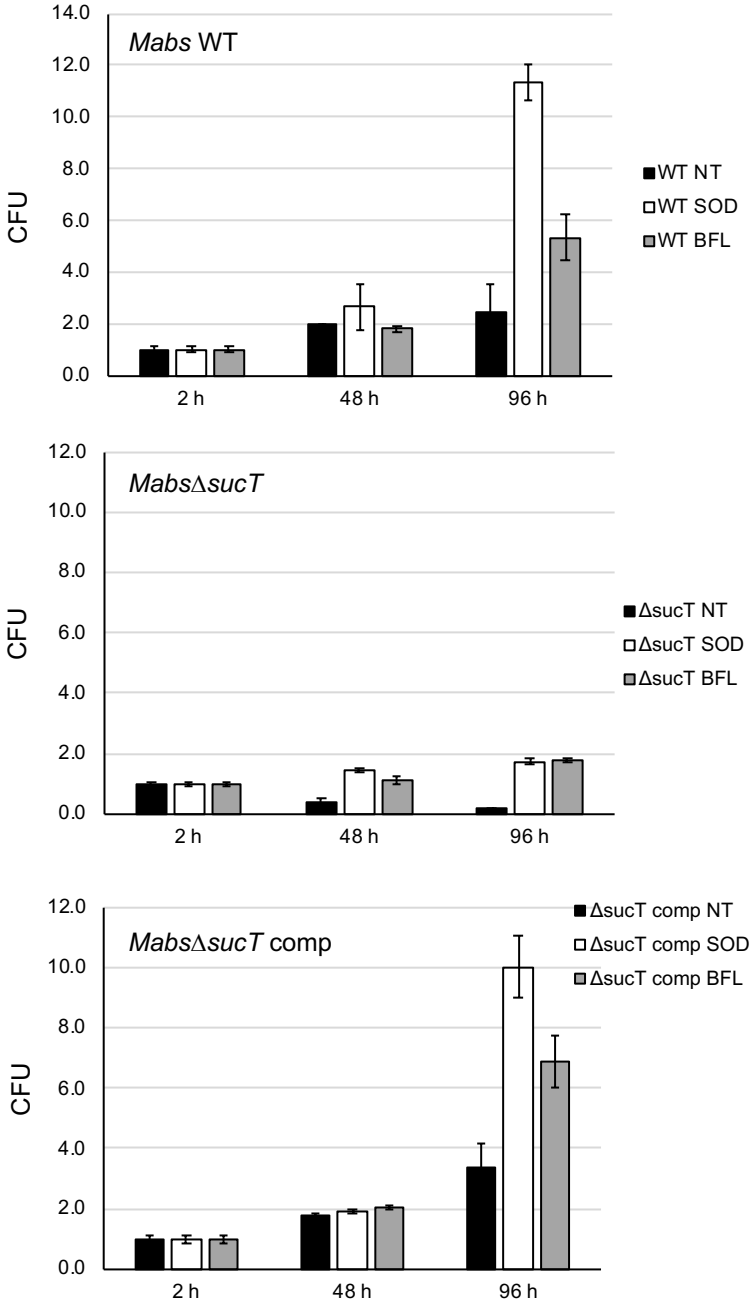

<u>Figure S8</u>: Effect of reactive oxygen species and phagosome acidification on the intracellular replication and survival of the *Mabs sucT* knock-out mutant.
Infected THP-1 macrophages were either non-treated (NT) or treated with superoxide dismutase (SOD) to inhibit superoxides, or treated with bafilomycin A1 (BFL) to inhibit vacuolar acidification. Intracellular CFU over time (average +/- SD of triplicate wells) were enumerated and are expressed relative to the number of CFU two hours post-infection for each treatment group arbitrarily set to 1. The results presented are representative of three independent experiments.